International Journal of Mechanical, Industrial and Aerospace Sciences
ISSN: 2517-9950
Vol:7, No:7, 2013

In-Plane Responses of Axially Moving Plates Subjected to Arbitrary Edge Excitations

T. H. Young and Y. S. Ciou

***Abstract*—**The free and forced in-plane vibrations of axially moving plates are investigated in this work. The plate possesses an internal damping of which the constitutive relation obeys the Kelvin-Voigt model, and the excitations are arbitrarily distributed on two opposite edges. First, the equations of motion and the boundary conditions of the axially moving plate are derived. Then, the extended Ritz method is used to obtain discretized system equations. Finally, numerical results for the natural frequencies and the mode shapes of the in-plane vibration and the in-plane response of the moving plate subjected to arbitrary edge excitations are presented. It is observed that the symmetry class of the mode shapes of the in-plane vibration disperses gradually as the moving speed gets higher, and the *u*- and *v*-components of the mode shapes belong to different symmetry class. In addition, large response amplitudes having shapes similar to the mode shapes of the plate can be excited by the edge excitations at the resonant frequencies and with the same symmetry class of distribution as the *u*-components.

***Keywords*—**Arbitrary edge excitations, axially moving plates, in-plane vibration, extended Ritz method.

I. Introduction

AXIALLY moving webs are frequently encountered applications in industries, such as magnetic tapes, driving belts, paper sheets, and plastic webs, etc. In order to raise production efficiency, the moving speed of the web gets faster and faster, which worsens the vibration problem of the web. Therefore, a vast number of researches concerning the dynamic behaviors of moving webs can be found in the literature [1]-[6]. Because the lowest natural frequency and critical speed of the out-of-plane vibration of the moving web are lower than those of the in-plane vibration, most of the references in literature deal with the out-of-plane vibration of the moving webs.

In literature, the references concerning the in-plane vibration of rectangular plates are much lesser than those pertaining to the out-of-plane vibration of rectangular plates. Hyde et al. [7] studied the free in-plane vibration of rectangular plates undergoing plane stress deformation through the Ritz discretization. The natural frequencies and mode shapes of rectangular plates with three different kinds of boundary conditions were presented in this work. The free in-plane vibrations of a rectangular plate under combined static pressure/tension edge loads were investigated by Wauer [8]. In this paper, the in-plane deformation due to static edge loads is determined first by solving the plane stress problem, and the free in-pane vibration is analyzed by the Rayleigh-Ritz method. A mathematical model was developed by Farag and Pan [9] for the prediction of the forced response of rectangular plates with all edges clamped to in-plane point force excitations. All the above three references dealt with the in-plane vibration of a stationary rectangular plate, and the references dealing with the in-plane vibration of axially moving rectangular plates are even less. Shin et al. [10] studied the free in-plane vibration of an axially moving plate by the Galerkin method. The elastic plate is subjected to a constant tension along two mass-transport boundaries, and two sets of boundary conditions, which are free and fixed constraints in the lateral direction at two mass-transport boundaries are discussed in this study.

To authors' knowledge, no research work on the in-plane response of axially moving plates subjected to arbitrary edge excitations can be found in the literature. Therefore, this work investigates the free and forced in-plane vibrations of axially moving plates. The plate possesses an internal damping of which the constitutive relation obeys the Kelvin-Voigt model, and the excitations are arbitrarily distributed on two opposite edges. First, the equations of motion and the boundary conditions of the axially moving plate are derived. Then, the extended Ritz method is used to obtain discretized system equations. Finally, numerical results for the natural frequencies and the mode shapes of the in-plane vibration and the in-plane response of the moving plate subjected to arbitrary edge excitations are presented.

II. Equations of Motion

Consider a rectangular plate of dimension $a \times b$ moving in the x-direction with a constant speed V. The plate is simply supported on two opposite edges $x = 0$ and a, and is free on the other two edges $y = 0$ and b. The plate is subjected to an excitation $f(y,t)$ arbitrarily distributed on two simply supported edges, as shown in Fig. 1. The plate possesses an internal damping of which the constitutive relation obeys the Kelvin-Voigt model, i.e.,

$$\sigma = E(\varepsilon + c\frac{\partial \varepsilon}{\partial t}) \tag{1}$$

where σ and ε are the stress and strain of the plate, respectively, and t is a temporal variable. E and c are Young's modulus and internal damping coefficient of the plate,

T. H. Young and Y. S. Ciou are with National Taiwan University of Science and Technology, Taipei 106, Taiwan (phone: 886-2-27376444; fax: 886-2-2737 6460; (e-mail: thyoung@mail.ntust.edu.tw, M10003122@ mail.ntust.edu. tw).

respectively. Therefore, the stress-strain relations for the plane stress state are given by

$$\sigma_x = \frac{E}{1-\nu^2}[(\varepsilon_x + \nu\varepsilon_y) + c(\frac{\partial \varepsilon_x}{\partial t} + \nu\frac{\partial \varepsilon_y}{\partial t})] \quad (2a)$$

$$\sigma_y = \frac{E}{1-\nu^2}[(\varepsilon_y + \nu\varepsilon_x) + c(\frac{\partial \varepsilon_y}{\partial t} + \nu\frac{\partial \varepsilon_x}{\partial t})] \quad (2b)$$

$$\sigma_{xy} = \frac{E}{1+\nu}[\varepsilon_{xy} + c\frac{\partial \varepsilon_{xy}}{\partial t}] \quad (2c)$$

where ν is Poisson's ratio of the plate. In terms of the in-plane displacement components, the strain energy of the plate can be expressed as

$$U = \frac{Eh}{2(1-\nu^2)}\int_0^a\int_0^b [(\frac{\partial u}{\partial x})^2 + (\frac{\partial v}{\partial y})^2 + 2\nu(\frac{\partial u}{\partial x})(\frac{\partial v}{\partial y}) + \frac{1-\nu}{2}(\frac{\partial u}{\partial y} + \frac{\partial v}{\partial x})^2]dxdy \quad (3)$$

where h is the thickness of the plate, and u and v are the in-plane displacement components of the plate in the x- and y-directions, respectively. The kinetic energy of the axially moving plate is given by

$$T = \frac{\rho h}{2}\int_0^a\int_0^b [(V + \frac{\partial u}{\partial t} + V\frac{\partial u}{\partial x})^2 + (\frac{\partial v}{\partial t} + V\frac{\partial v}{\partial x})^2]dxdy \quad (4)$$

where ρ is the mass density of the plate. The virtual work done by the edge excitation is written as

$$\delta W_K = \int_0^b f(y,t)[\delta u|_{x=a} - \delta u|_{x=0}]dy \quad (5)$$

The virtual work done by the internal damping force is given by

$$\delta W_d = -\frac{Ehc}{1-\nu^2}\int_0^a\int_0^b [(\frac{\partial^2 u}{\partial t\partial x} + \nu\frac{\partial^2 v}{\partial t\partial y})\delta(\frac{\partial u}{\partial x}) + (\frac{\partial^2 v}{\partial t\partial y} + \nu\frac{\partial^2 u}{\partial t\partial x})\delta(\frac{\partial v}{\partial y}) + \frac{1-\nu}{2}(\frac{\partial^2 u}{\partial t\partial y} + \frac{\partial^2 v}{\partial t\partial x})\delta(\frac{\partial u}{\partial y} + \frac{\partial v}{\partial x})]dxdy \quad (6)$$

The virtual work done by the momentum of the plate moving across the boundaries is found to be

$$\delta M_v = \int_0^b \rho hV[(V + \frac{\partial u}{\partial t} + V\frac{\partial u}{\partial x})\delta u|_0^a + (\frac{\partial v}{\partial t} + V\frac{\partial v}{\partial x})\delta v|_0^a]dy \quad (7)$$

The extended Hamilton principle for non-conservative systems requires

$$\int_{t1}^{t2}(\delta T - \delta U + \delta W_k + \delta W_d - \delta M_v)dt = 0 \quad (8)$$

where t_1 and t_2 are two time instants at which the virtual displacements δu and δv vanish. Substituting (3) – (7) into (8) and going through variational calculus manipulations yield the equations of motion and boundary conditions for the axially moving plate,

$$\rho h(\frac{\partial^2 u}{\partial t^2} + 2V\frac{\partial^2 u}{\partial t\partial x} + V^2\frac{\partial^2 u}{\partial x^2}) - \frac{Eh}{1-\nu^2}(\frac{\partial^2 u}{\partial x^2} + \nu\frac{\partial^2 v}{\partial x\partial y}) - \frac{Eh}{2(1+\nu)}(\frac{\partial^2 u}{\partial y^2} + \frac{\partial^2 v}{\partial x\partial y}) - \frac{Ehc}{1-\nu^2}\frac{\partial}{\partial t}(\frac{\partial^2 u}{\partial x^2} + \nu\frac{\partial^2 v}{\partial x\partial y}) - \frac{Ehc}{2(1+\nu)}\frac{\partial}{\partial t}(\frac{\partial^2 u}{\partial y^2} + \frac{\partial^2 v}{\partial x\partial y}) = f(y,t)[\delta(x-a) - \delta(x)] \quad (9a)$$

$$\rho h(\frac{\partial^2 v}{\partial t^2} + 2V\frac{\partial^2 v}{\partial t\partial x} + V^2\frac{\partial^2 v}{\partial x^2}) - \frac{Eh}{1-\nu^2}(\frac{\partial^2 v}{\partial y^2} + \nu\frac{\partial^2 u}{\partial x\partial y}) - \frac{Eh}{2(1+\nu)}(\frac{\partial^2 v}{\partial x^2} + \frac{\partial^2 u}{\partial x\partial y}) - \frac{Ehc}{1-\nu^2}\frac{\partial}{\partial t}(\frac{\partial^2 v}{\partial y^2} + \nu\frac{\partial^2 u}{\partial x\partial y}) - \frac{Ehc}{2(1+\nu)}\frac{\partial}{\partial t}(\frac{\partial^2 v}{\partial x^2} + \frac{\partial^2 u}{\partial x\partial y}) = 0 \quad (9b)$$

$$\text{at } x = 0 \text{ and } a,\ N_x = 0 \text{ and } v = 0 \quad (10a)$$

$$\text{at } y = 0 \text{ and } b,\ N_y = 0 \text{ and } N_{xy} = 0 \quad (10b)$$

where N_x, N_y, and N_{xy} are the in-plane stress resultants of the plate. Equations (10a) and (10b) can be reduced to those obtained by Shin et al. [10] if the internal damping force terms are deleted.

Equations (10a) and (10b) constitute a system of the second order partial differential equations in terms of the displacement components u and v. Since the exact solution of them is not feasible, to obtain approximate solutions in the finite dimensional space, discretization of the system equations is carried out. Due to the boundary conditions of the problem, it is very difficult to find the comparison functions, the ones that satisfy both the geometric and natural boundary conditions, as the trial functions. Therefore, the extended Ritz method, which admits the admissible functions satisfying the geometric boundary conditions only as the trial functions, is adopted in conjunction with the extended Hamilton principle. Assume the displacement components u and v to be of the forms,

$$u(x,y,t) = \sum_{m=0}^{M}\sum_{n=0}^{N} A_{mn}(t)(\frac{x}{a})^m(\frac{y}{b})^n, \quad (11a)$$

$$v(x,y,t) = \sum_{m=0}^{M}\sum_{n=0}^{N} B_{mn}(t)\sin\frac{(m+1)\pi x}{a}(\frac{y}{b})^n \quad (11b)$$

where $A_{mn}(t)$ and $B_{mn}(t)$ are undetermined functions. Substituting (11a) and (11b) into (8) and non- dimensionalizing all parameters and variables yield the following equation,

$$[M]U'' + (\widetilde{V}[G] + \widetilde{c}[K_e])U' + ([K_e] + \widetilde{V}^2[K_g])U = F(\tau) \quad (12)$$

where the non-dimensional parameters $\widetilde{V} = V\sqrt{\frac{(1-\nu^2)\rho a^2}{E}}$, $\widetilde{c} = c\sqrt{\frac{E}{(1-\nu^2)\rho a^2}}$, $\tau = t\sqrt{\frac{E}{(1-\nu^2)\rho a^2}}$, and a prime denotes a differentiation with respect to τ. The mass matrix $[M]$, the moving-speed dependent matrix $[G]$, the elastic stiffness matrix $[K_e]$, and the geometric stiffness matrix $[K_g]$ have the following forms,

$$[M] = \begin{bmatrix} [M_u] & [0] \\ [0] & [M_v] \end{bmatrix}, \qquad [G] = \begin{bmatrix} [G_u] & [0] \\ [0] & [G_v] \end{bmatrix},$$
$$[K_e] = \begin{bmatrix} [K_{uu}] & [K_{uv}] \\ [K_{vu}] & [K_{vv}] \end{bmatrix}, \qquad [K_g] = \begin{bmatrix} [K_{gu}] & [0] \\ [0] & [K_{gv}] \end{bmatrix},$$

in which the block matrices $[M_u]$, $[M_v]$, $[K_{uu}]$, and $[K_{vv}]$ are symmetric, and $[K_{uv}]^T = [K_{vu}]$. Therefore, the mass matrix $[M]$ and the elastic stiffness matrix $[K_e]$ are symmetric, the moving-speed dependent matrix $[G]$ and the geometric stiffness matrix $[K_g]$ are neither symmetric nor skew-symmetric. The response vector U and the forcing vector $F(\tau)$ in (12) have the following forms,

$$U = \begin{bmatrix} A \\ B \end{bmatrix}, \qquad F(\tau) = \begin{bmatrix} f(\tau) \\ 0 \end{bmatrix}$$

where A and B are column matrices formed by all $A_{mn}(\tau)/b$ and $B_{mn}(\tau)/b$, and $f(\tau)$ is a column matrix.

Equation (12) governs the in-plane forced response of an axially moving plate. To find the natural frequencies and the mode shapes of the free in-plane vibration, neglect the nonhomogeneous forcing term on the right-hand side of the equation, and rewritten the set of the second order differential equations into a set of first order differential equations, which yield the following eigenvalue problem,

$$s\begin{bmatrix} [M] & [0] \\ [0] & [I] \end{bmatrix} Z + \begin{bmatrix} (\widetilde{V}[G] + \widetilde{c}[K_e]) & ([K_e] + \widetilde{V}^2[K_g]) \\ -[I] & [0] \end{bmatrix} Z = 0 \quad (13)$$

where $[I]$ is an identity matrix. The eigenvalues of the above equation are in pairs of complex conjugates, $s_{2j-1,2j} = \lambda_j \pm i\omega_j$, j=1, 2, …, L, where $L = 2(M+1)(N+1)$ is the total degrees of freedom of the discretized system. The eigenvectors of the above equation are also in pairs of complex conjugates, $Z_{2j-1,2j} = X_j \pm iY_j$, j=1, 2, …, L. The imaginary part of the eigenvalue ω_j is the non- dimensionalized natural frequency of the jth mode of the axially moving plate, while $\varsigma_j = -\lambda_j/\omega_j$ is the damping ratio of the jth mode of the axially moving plate. If the real parts of all eigenvalues are smaller than or equal to 0, the axially moving plate is stable; otherwise, the axially moving plate is unstable. Therefore, the critical speeds for the in-plane vibration of the plate can be obtained when the real part of one eigenvalue becomes positive.

To calculate the in-plane forced response of the axially moving plate, assume the edge excitation is simply harmonic in time, i.e., $f(y,t) = q(y)\sin\Omega t$, where Ω is the exciting frequency. The forcing vector $F(\tau)$ in (12) will have the form $F(\tau) = Q_0 \sin\widetilde{\Omega}\tau$, where Q_0 is a constant vector, and $\widetilde{\Omega} = \Omega\sqrt{(1-\nu^2)\rho a^2/E}$. To match the form of the forcing vector, assume the response vector to be of the form,

$$U(\tau) = U_s \sin\widetilde{\Omega}\tau + U_c \cos\widetilde{\Omega}\tau \quad (14)$$

where U_s and U_c are the sine and cosine components of the response vector, respectively. Substituting (14) into (12) yields the following equation,

$$\begin{bmatrix} ([K_e] + \widetilde{V}^2[K_g] - \widetilde{\Omega}^2[M]) & -\widetilde{\Omega}(\widetilde{V}[G] + \widetilde{c}[K_e]) \\ \widetilde{\Omega}(\widetilde{V}[G] + \widetilde{c}[K_e]) & ([K_e] + \widetilde{V}^2[K_g] - \widetilde{\Omega}^2[M]) \end{bmatrix} \begin{bmatrix} U_s \\ U_c \end{bmatrix} = \begin{bmatrix} Q_0 \\ 0 \end{bmatrix} \quad (15)$$

Once U_s and U_s are solved, the functions $A_{mn}(\tau)$ and $B_{mn}(\tau)$ are determined, from which the in-plane responses u and v are calculated. Since the response vector contains the sine and cosine components, the functions $A_{mn}(\tau)$ and $B_{mn}(\tau)$ consist of the sine and cosine components also, i.e.,

$$\frac{A_{mn}(\tau)}{b} = A_{mn}^s \sin\widetilde{\Omega}\tau + A_{mn}^c \cos\widetilde{\Omega}\tau \quad (16a)$$

$$\frac{B_{mn}(\tau)}{b} = B_{mn}^s \sin\widetilde{\Omega}\tau + B_{mn}^c \cos\widetilde{\Omega}\tau \quad (16b)$$

where A_{mn}^s, A_{mn}^c, B_{mn}^s, and B_{mn}^c are constants. The responses u and v can be written in the amplitude-phase angle form,

$$\widetilde{u}(\xi,\eta,\tau) = C_u(\xi,\eta)\sin(\widetilde{\Omega}\tau - \phi_u) \quad (17a)$$

$$\widetilde{v}(\xi,\eta,\tau) = C_v(\xi,\eta)\sin(\widetilde{\Omega}\tau - \phi_v) \quad (17b)$$

where the amplitudes

$$C_u(\xi,\eta)=\sqrt{[\sum_{m=0}^{M}\sum_{n=0}^{N}A_{mn}^{s}(\frac{x}{a})^m(\frac{y}{b})^n]^2+[\sum_{m=0}^{M}\sum_{n=0}^{N}A_{mn}^{c}(\frac{x}{a})^m(\frac{y}{b})^n]^2}$$

$$C_v(\xi,\eta)=\sqrt{[\sum_{m=0}^{M}\sum_{n=0}^{N}B_{mn}^{s}\sin\frac{(m+1)\pi x}{a}(\frac{y}{b})^n]^2+[\sum_{m=0}^{M}\sum_{n=0}^{N}B_{mn}^{c}\sin\frac{(m+1)\pi x}{a}(\frac{y}{b})^n]^2}$$

and the phase angles

$$\phi_u=\tan^{-1}\frac{\sum_{m=0}^{M}\sum_{n=0}^{N}A_{mn}^{s}(\frac{x}{a})^m(\frac{y}{b})^n}{\sum_{m=0}^{M}\sum_{n=0}^{N}A_{mn}^{c}(\frac{x}{a})^m(\frac{y}{b})^n}$$

$$\phi_v=\tan^{-1}\frac{\sum_{m=0}^{M}\sum_{n=0}^{N}B_{mn}^{s}\sin\frac{(m+1)\pi x}{a}(\frac{y}{b})^n}{\sum_{m=0}^{M}\sum_{n=0}^{N}B_{mn}^{c}\sin\frac{(m+1)\pi x}{a}(\frac{y}{b})^n}$$

III. Numerical Results

A. Free Vibration

In order to verify the correctness of the results obtained in this work, comparison is carried out with the results by Shin et al. [10]. Table I presents the lowest six natural frequencies of an axially moving rectangular plate without internal damping. It is observed that with M=N=8, the numerical results obtained in this work agree excellently with those reported in the reference [10]. The maximum difference between these two sets of results using the same degrees of freedom is about 0.05%. Fig. 2 illustrates the lowest six mode shapes of an axially moving rectangular plate with internal damping. The u-component and the v-component of each mode shape are drawn in different plots, respectively. Since the moving speed of the plate is very low, the mode shapes almost preserve the symmetry class that is owned only by stationary plates. The figure shows that the u-components of the first and the fourth mode shapes are anti-symmetric in both the x- and y-directions. The u-components of the second and the fifth mode shapes are symmetric in the x-direction and are anti- symmetric in the y-direction. The u-component of the third mode shape is anti-symmetric in the x-direction and is symmetric in the y-direction, while that of the sixth mode shape is symmetric in both the x- and y-directions. The figure shows the opposite trend for the v-components. Moreover, the fifth mode shape of the axially moving rectangular plate is a purely u-component mode. The symmetry class of the mode shapes disperses gradually as the moving speed of the plate becomes higher because the moving–speed dependent matrix and the geometric stiffness matrix are neither symmetric nor skew-symmetric.

Table II shows the lowest six natural frequencies and modal damping ratios of an axially moving rectangular plate with internal damping. It is found that the natural frequencies of the plate with internal damping are slightly lower than those of the plate without internal damping, and the modal damping ratio is monotonically increasing for higher modes. Fig. 3 depicts the real and the imaginary parts of the eigenvalues of the lowest seven modes of an axially moving rectangular plate with internal damping. In Fig. 3 (a), all the imaginary parts of the eigenvalues, which are the natural frequencies of the axially moving plate, drop as the moving speeds of the plate increase. At $\widetilde{V}$ =0.2486, the imaginary part of the lowest mode reduces to zero. Moreover, veering phenomena occur when the imaginary part of the seventh mode meets that of the sixth mode at $\widetilde{V}$ =0.1587; when the imaginary part of the sixth mode meets that of the fifth mode at $\widetilde{V}$ =0.1637, and when the imaginary part of the sixth mode meets that of the seventh mode at $\widetilde{V}$ =0.1686. In Fig. 3 (b), all the real parts of the eigenvalues are negative and hold nearly constant except the followings. The real part of the lowest mode rises and becomes positive at the speed which the imaginary part of the lowest mode reduces to zero. That is the moving plate becomes unstable at this speed, and this speed is called the first critical speed of the moving plate. The real parts of the fifth, sixth and seventh modes jump up and down respectively, and cross each other at the speeds where veering phenomena occur. Because the internal damping of the plate in this figure is small, Fig. 3 (a) looks very similar to that obtained by Shin et al. [10] in which no internal damping is considered.

B. Forced Vibration

Fig. 4 illustrates the forced response of an axially moving plate subjected to excitations uniformly distributed on two simply supported edges at zero and the lowest five resonant frequencies. All u-components of the response plots in the figure are nearly anti-symmetric in the axial direction and are nearly symmetric in the lateral direction, whereas all v-components of the response plots show the opposite symmetry class, that is, nearly symmetric in the axial direction and nearly anti-symmetric in the lateral direction. This trend loses gradually for higher resonant frequencies. Because the response plots possess the same symmetry class of the third mode, the amplitudes of the response plot at the third resonant frequency are one-order larger than those at the other resonant frequencies. Except for that, the response amplitudes generally reduce gradually as the resonant frequencies get higher, and the static deformation of the plate subjected to static edge loads are close to the forced response amplitudes at the first resonant frequency.

Fig. 5 shows the forced response of an axially moving plate subjected to excitations linearly distributed on two simply supported edges such that the distribution of the excitations are anti-symmetric in the lateral direction. All u-components of the response plots in the figure are almost anti-symmetric in both axial and lateral directions, whereas all v-components of the response plots are almost symmetric in both directions. Again, this trend loses gradually for higher resonant frequencies. Because the response plots possess the same symmetry class of

the first and the fourth modes, the amplitudes of the response plot at the first resonant frequency are at least two-order larger than those at the other resonant frequencies, and the amplitudes of the response plot at the fourth resonant frequency are larger than those at the second and the third resonant frequencies. The response plot at the first resonant frequency is similar to the static deformation plot subjected to static edge loads, and the response amplitudes at the first resonant frequency are about one hundred times of the static deformation subjected to static edge loads, which is the inverse of the internal damping factor $\tilde{c}$. Note that the amplitudes of the response plot at the first resonant frequency in this figure are even larger than those of the plate subjected to uniformly distributed edge excitations at the third resonant frequency, as shown in Fig. 3 (c).

The forced response of an axially moving plate subjected to excitations linearly, anti-symmetrically distributed on the middle halves of two simply supported edges is depicted in Fig. 6. The distribution of the excitations is again anti- symmetric in the lateral direction, and the intensity of the excitation is twice as that in Fig. 5. All corresponding plots in both figures look similar, but the amplitudes in this figure are a little bit smaller than those in the previous figure.

The effect of the internal damping on the forced response of an axially moving plate is shown in Fig. 7. In this figure, the forced response of the plate considered in Fig. 5 but with a larger internal damping factor is illustrated. Comparing between both figures, it is observed that the response plots in both figures look similar, and the response plots at the first, the second, and the fourth resonant frequencies in this figure deviate more from the mode shapes of the plate than the corresponding plots in Fig. 5. Because the response plots possess the same symmetry class of the first and the fourth modes, the amplitude ratios between Figs. 5 and 7 at the first and the fourth resonant frequencies are about 10:1, which is approximately inversely proportional to the internal damping ratio between these two figures. But the amplitudes between these two figures at the other resonant frequencies are of the same orders.

The effect of the aspect ratio on the forced response of an axially moving plate is presented in Fig. 8. In this figure, the forced response of a square plate is considered. Because the aspect ratio of the plate is smaller, the natural frequencies of the plate rise and the mode shapes of the plate change also. The *u*-component of the first mode shape is anti-symmetric in both the *x*- and *y*-directions. The *u*-components of the second and the fourth mode shapes are symmetric in the *x*-direction and are anti-symmetric in the *y*-direction. The *u*-components of the third and the fifth mode shapes are anti-symmetric in the *x*-direction and are symmetric in the *y*-direction. The *v*-components of the mode shapes have the opposite class of symmetry. Because the distribution of the edge excitation is linear, anti-symmetric in the lateral direction, the amplitudes of the response at the first resonant frequency is the highest among those at the lowest five resonant frequencies. In addition, the amplitudes of the response at the first resonant frequency in this figure are much smaller than those at the first resonant frequency in Fig. 5 (a) because the aspect ratio of the plate in this figure is smaller than that of the plate considered in Fig. 5, and hence the plate considered in this figure is more stiffer.

IV. Conclusions

The free and forced in-plane vibrations of axially moving plates subjected to arbitrarily distributed edge excitations on two opposite, simply-supported edges are studied by the extended Ritz method in this work. Numerical results for the natural frequencies, mode shapes and the critical speed of the free in-plane vibration and the response amplitudes of the forced in-plane vibration are presented for different system parameters and the distribution of the edge excitations. The numerical results for the natural frequencies, mode shapes and the critical speed of the free in-plane vibration are compared with [10], and excellent agreement of the numerical results between these two works is observed. From these numerical results, the following conclusions can be drawn:

1) The mode shapes of the corresponding stationary plate preserve symmetry class, and the *u*-components and *v*-components of the mode shapes belong to the opposite symmetry class. The symmetry class of the mode shapes of the free in-plane vibration disperses gradually as the moving speed of the plate becomes higher.
2) The natural frequencies of the plate with internal damping are slightly lower than those of the plate without internal damping, and the modal damping ratio is monotonically increasing for higher modes.
3) At the first critical speed, the imaginary part of the lowest mode reduces to zero, and the real part of the lowest mode becomes positive. Veering phenomena occur among the fifth, sixth and seventh modes when two imaginary parts of these modes meet each other, and the real parts of these modes jump up and down respectively and cross each other at the speeds where veering phenomena occur.
4) For an axially moving plate subjected to excitations symmetrically distributed in the lateral direction on two simply supported edges, all *u*-components of the response plots are nearly anti-symmetric in the axial direction and are nearly symmetric in the lateral direction. For an axially moving plate subjected to excitations anti-symmetrically distributed in the lateral direction on two simply supported edges, all *u*-components of the response plots are nearly anti-symmetric in both the axial and the lateral directions. The *v*-components of the response plots show the opposite symmetry class. This trend loses gradually for higher resonant frequencies and faster moving speeds.
5) If the response plot possesses the same symmetry class as the mode shape of a mode, the amplitudes of the response plot at that resonant frequency will be much larger than those at the other resonant frequencies. Except for that, the response amplitudes generally reduce gradually as the resonant frequencies get higher.
6) The effect of the internal damping is very effective only when the symmetry class of the edge excitation meets the

same symmetry class of the mode shape at that resonant frequency. Otherwise, its effect is insignificant.

TABLE I
THE NATURAL FREQUENCIES OF AN UNDAMPED AXIALLY MOVING PLATE
$a/b=3, \widetilde{V}=0.1, \widetilde{c}=0$

Mode no.	1	2	3	4	5	6
Present work	0.6937	2.2885	2.9494	4.0641	5.5758	5.7422
[10]	0.6937	2.2882	2.9493	4.0619	5.5758	5.7419
Error	0%	0.0131 %	0.0034 %	0.0542 %	0%	0.0052 %

TABLE II
THE NATURAL FREQUENCIES AND MODAL DAMPING RATIOS OF A DAMPED AXIALLY MOVING PLATE
$a/b=3, \widetilde{V}=0.1, \widetilde{c}=0.01$

Mode no.	1	2	3	4	5	6
ω_j	0.6937	2.2883	2.9490	4.0631	5.5736	5.7397
ς_j	0.0022	0.0063	0.0075	0.011	0.0139	0.0148

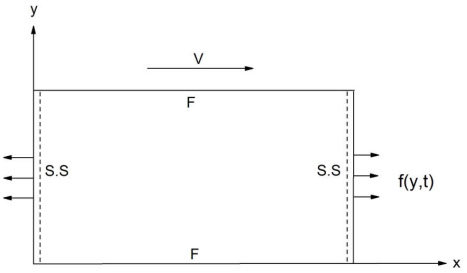

Fig. 1 An axially moving plate subjected to arbitrarily distributed excitations

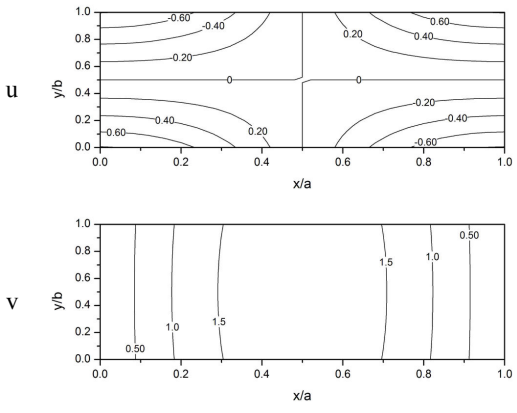

(a) 1st mode

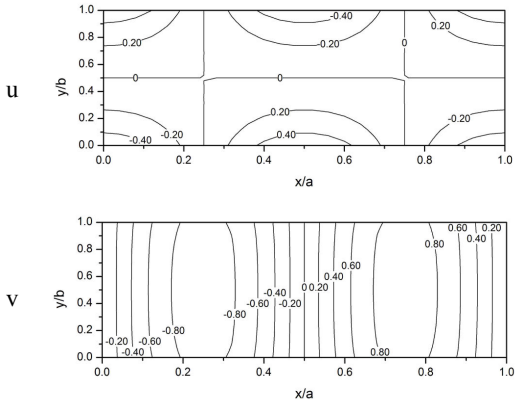

(b) 2nd mode

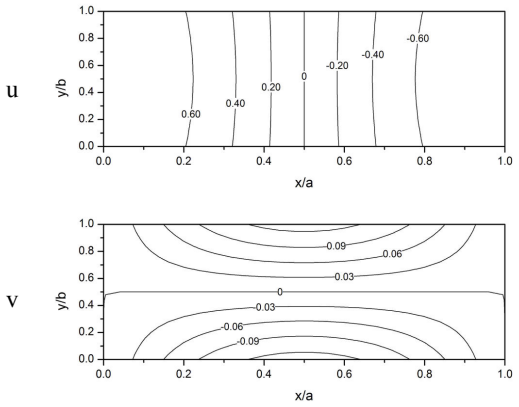

(c) 3rd mode

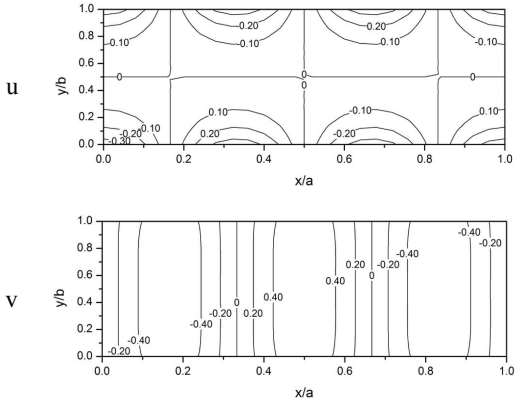

(d) 4th mode

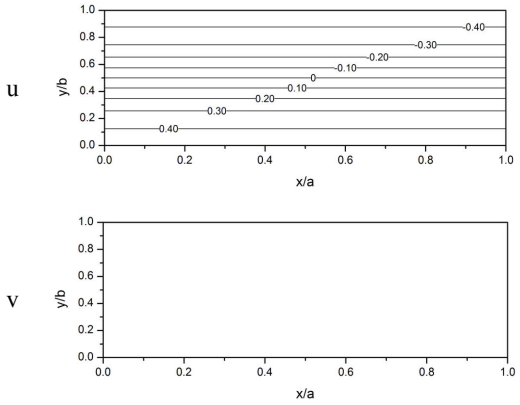

(e) 5th mode

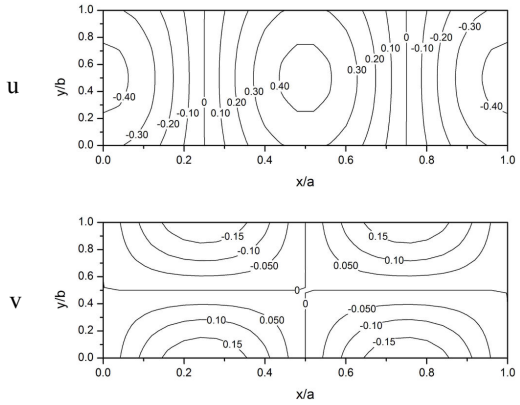

(f) 6th mode

Fig. 2 The mode shapes of a damped axially moving plate $a/b=3, \widetilde{V}=0.01, \widetilde{c}=0.01$

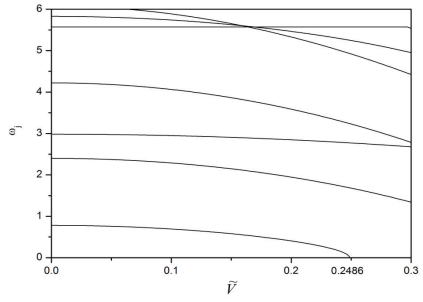

(a) Imaginary part

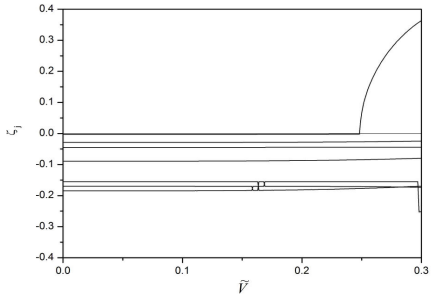

(b) Real part

Fig. 3 The eigenvalues curves of the lowest seven modes of an axially moving plate $a/b=3, \widetilde{c}=0.01$

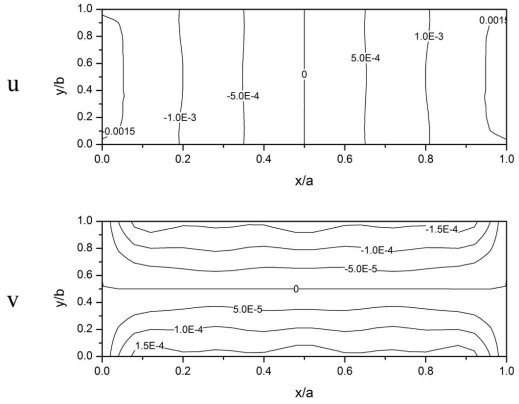

(a) $\Omega/\omega_1=0$

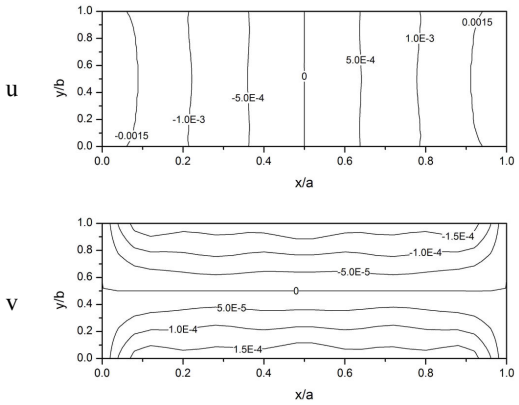

(b) $\Omega/\omega_1=0.9999$

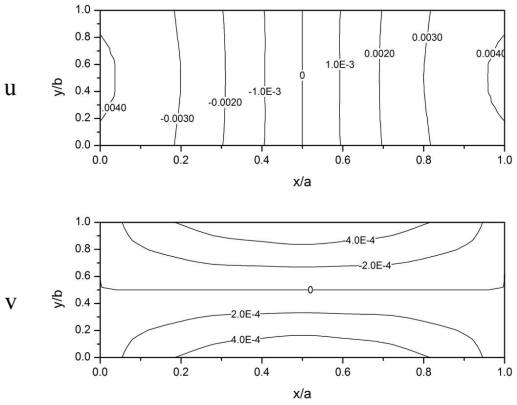

(c) Ω/ω_1 =3.0749

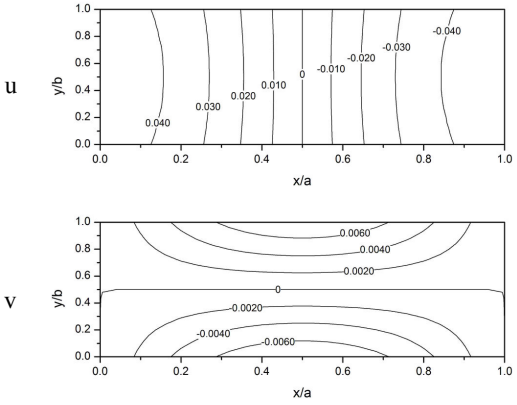

(d) Ω/ω_1 =3.8237

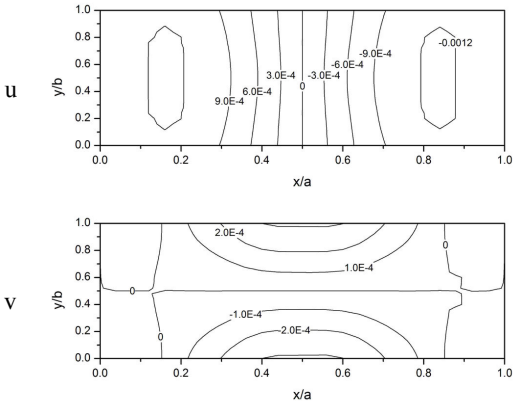

(e) Ω/ω_1 =5.4108

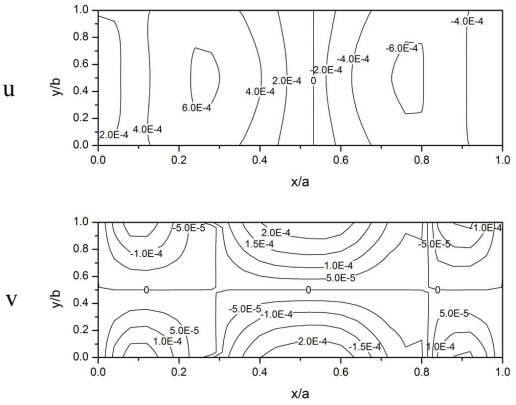

(f) Ω/ω_1 =7.1456

Fig. 4 The forced response plots of an axially moving plate subjected to uniformly distributed excitations a/b =3, $\tilde{V}$ =0.01, $\tilde{c}$ =0.01

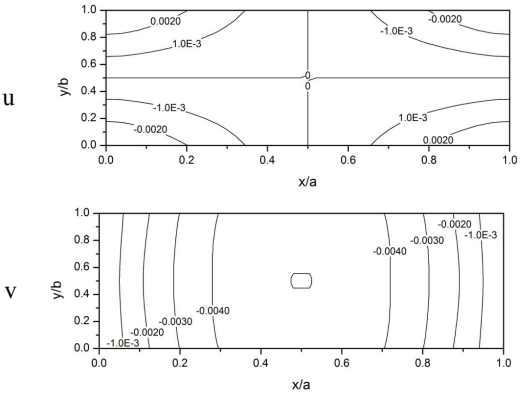

(a) Ω/ω_1 =0

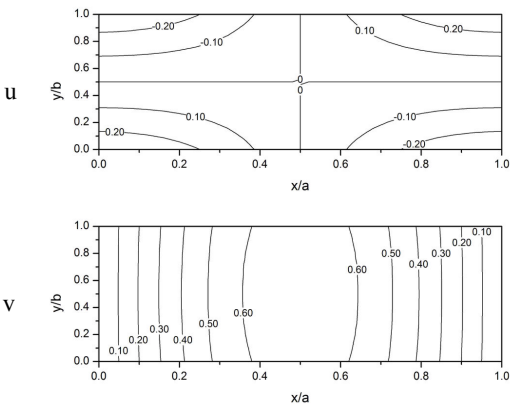

(b) Ω/ω_1 =0.9999

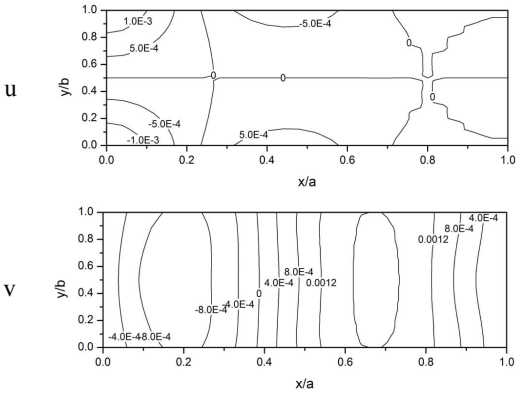

(c) Ω/ω_1 =3.0749

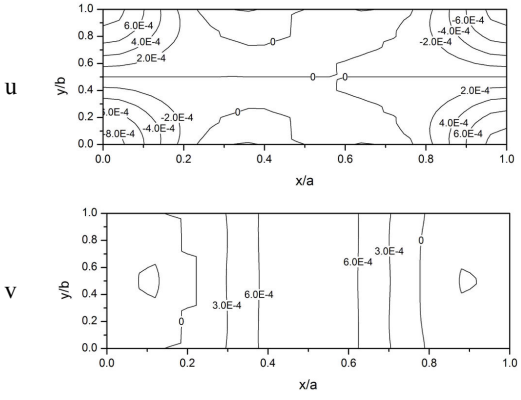

(d) Ω/ω_1 =3.8237

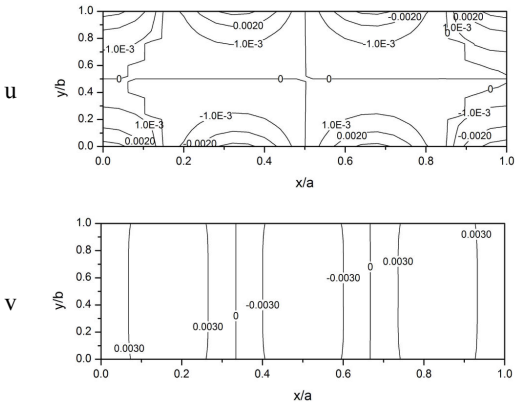

(e) Ω/ω_1 =5.4108

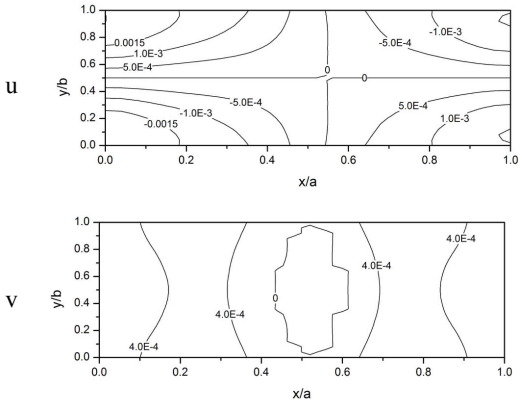

(f) Ω/ω_1 =7.1456

Fig. 5 The forced response plots of an axially moving plate subjected to linearly, anti-symmetrically distributed excitations a/b =3, $\widetilde{V}$ =0.01, $\widetilde{c}$ =0.01

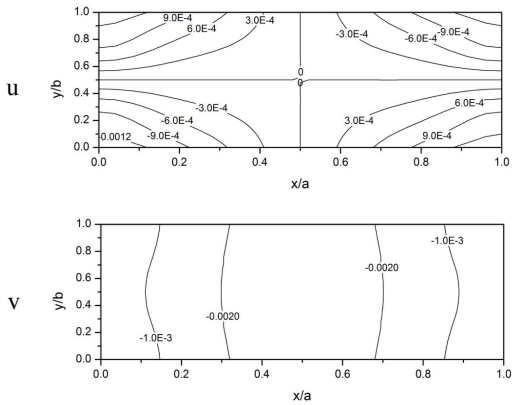

(a) Ω/ω_1 =0

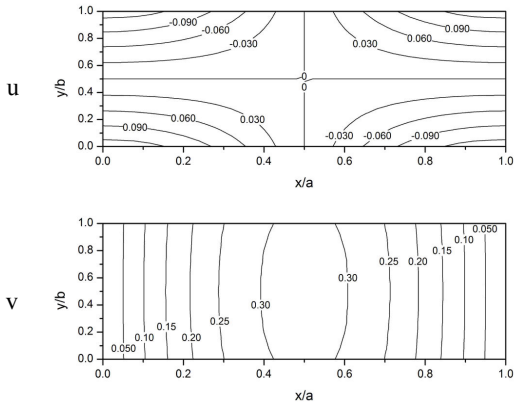

(b) Ω/ω_1 =0.9999

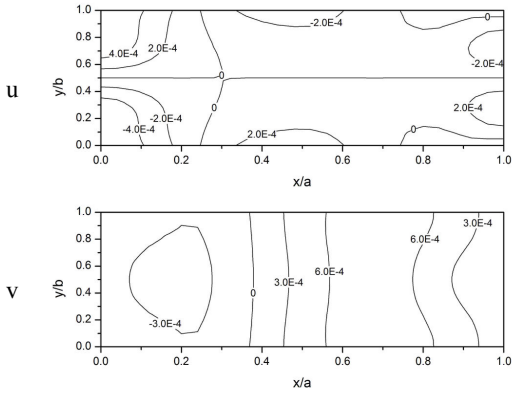

(c) Ω/ω_1 =3.0749

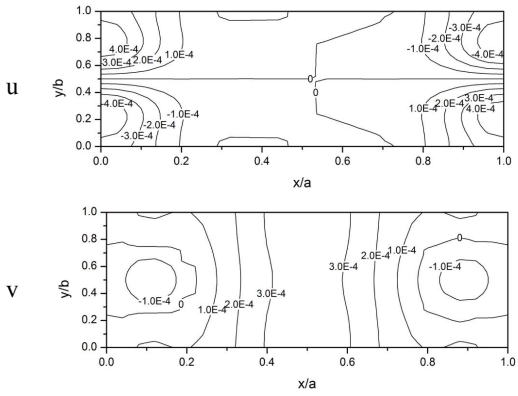

(d) Ω/ω_1 =3.8237

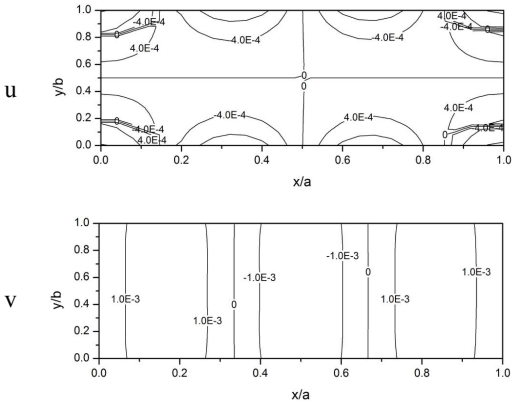

(e) Ω/ω_1 =5.4108

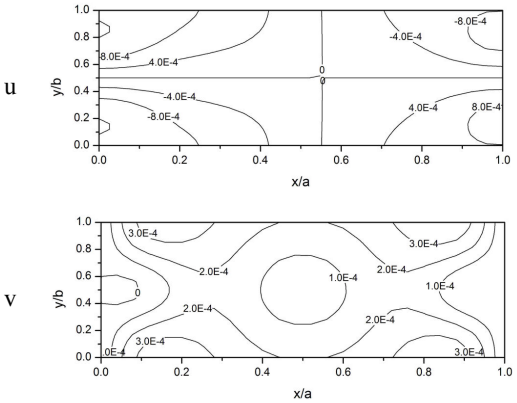

(f) Ω/ω_1 =7.1456

Fig. 6 The forced response plots of an axially moving plate subjected to excitations linearly, anti-symmetrically distributed on the middle halves of the edges a/b =3, $\widetilde{V}$ =0.01, $\widetilde{c}$ =0.01

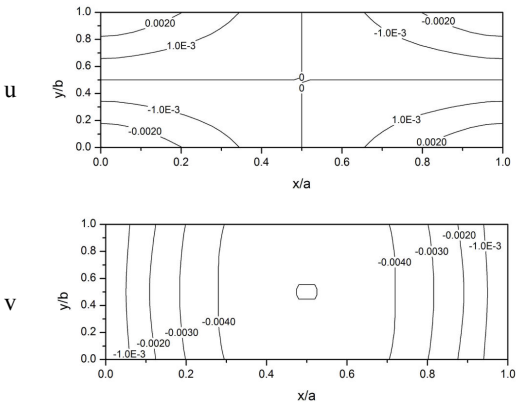

(a) Ω/ω_1 =0

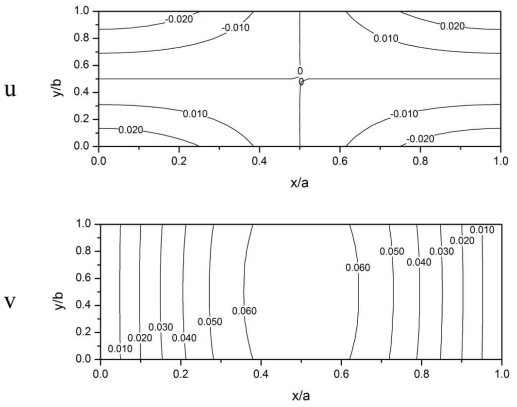

(b) Ω/ω_1 =0.9992

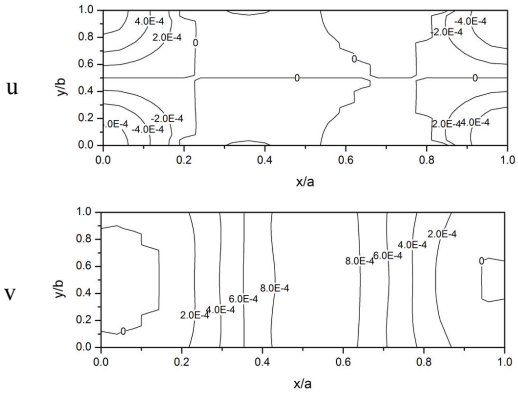

(c) Ω/ω_1 =3.0529

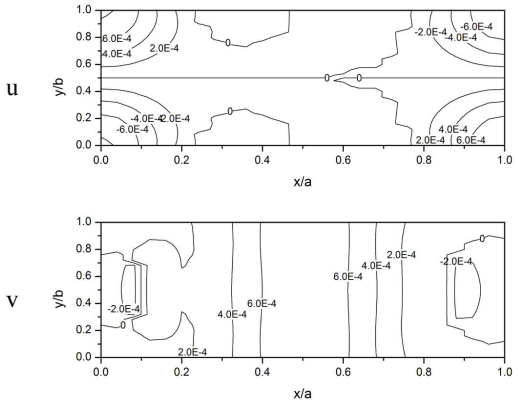

(d) Ω/ω_1 =3.7813

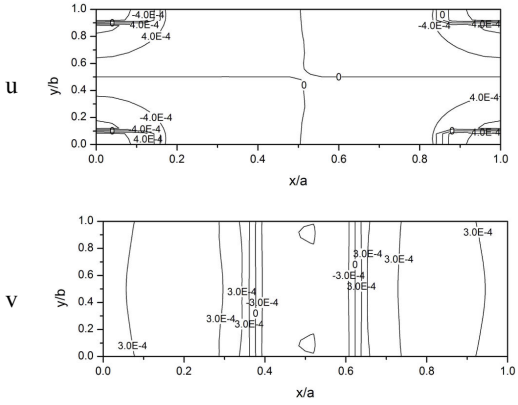

(e) Ω/ω_1 =5.2899

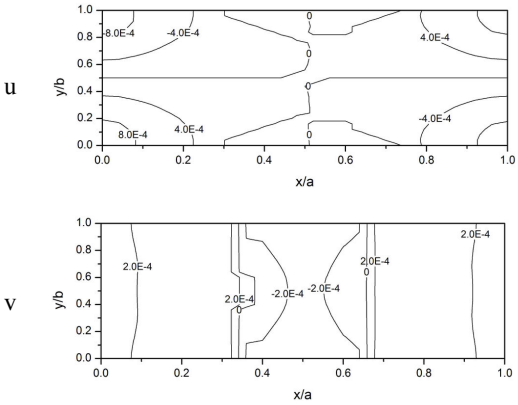

(f) Ω/ω_1 =6.8650

Fig 7 The forced response plots of an axially moving plate subjected to linearly, anti-symmetrically distributed excitations a/b =3, $\widetilde{V}$ =0.01, $\widetilde{c}$ =0.1

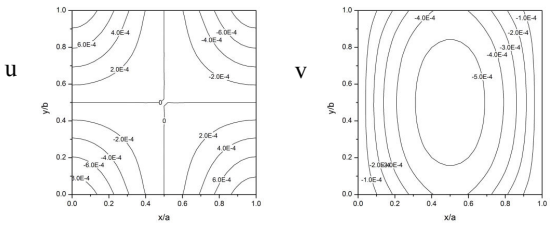

(a) Ω/ω_1 =0

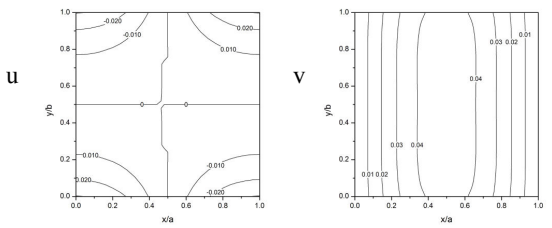

(b) Ω/ω_1 =1.0

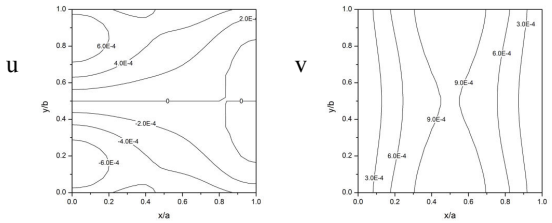

(c) Ω/ω_1 =1.321

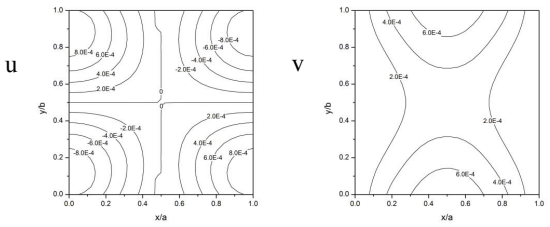

(d) Ω/ω_1 =1.8677

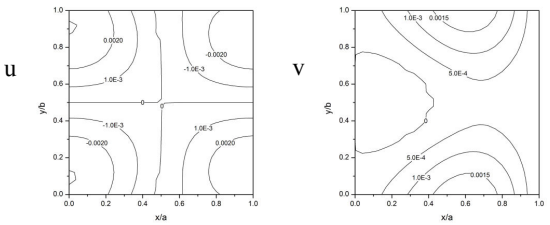

(e) Ω/ω_1 =2.3079

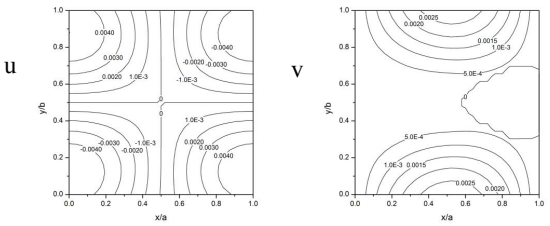

(f) Ω/ω_1 =2.3901

Fig. 8 The forced response plots of an axially moving plate subjected to linearly, anti-symmetrically distributed excitations $a/b=1, \widetilde{V}=0.01, \widetilde{c}=0.01$

REFERENCES

[1] F. Fung, J. S. Huang, and Y. C. Chen, "The transient amplitude of the viscoelastic travelling string: An integral constitutive law," *Journal of Sound and Vibration*, vol. 201, pp. 153-167, 1997.

[2] L. Q. Chen, and X. D. Yang, "Steady-state response of axially moving viscoelastic beams with pulsating speed: comparison of two nonlinear models," *International Journal of Solids and Structures*, vol. 42, pp. 35-50, 2005.

[3] C. Shin, J. Chung, and W. Kim, "Dynamic characteristics of the out-of-plane vibrations for an axially moving membrane," *Journal of Sound and Vibration*, vol. 297, pp. 794-809, 2006.

[4] K. Marynowski, "Two-dimensional rheological element in modeling of axially moving viscoelastic web," *European Journal of Mechanics – A/Solids*, vol. 25, pp. 729-744, 2006.

[5] C. C. Lin, "Stability and vibration characteristics of axially moving plates," *International Journal of Solids and Structures*, vol. 34, pp. 3179-3190, 1997.

[6] S. Hatami, H. R. Ronagh, and M. Azhari, "Exact free vibration analysis of axially moving viscoelastic plates," *Computers & Structures*, vol. 86, pp. 1734-1746, 2008.

[7] K. Hyde, J. Y. Chang, C. Bacca, and J. A. Wickert, "Parameter studies for plane stress in-plane vibration of rectangular plates," *Journal of Sound and Vibration*, vol. 247, pp. 471-487, 2001.

[8] J. Wauer, "In-plane vibrations of rectangular plates under inhomogeneous static edge load," *European Journal of Mechanics – A/Solids*, vol. 11, pp. 91-106, 1992.

[9] N. H. Farag, and J. Pan, "Free and forced in-plane vibration of rectangular plates," *Journal of Acoustical Society of America*, vol. 103, pp. 408-413, 1998.

[10] C. Shin, W. Kim, and J. Chung, "Free in-plane vibration of an axially moving membrane," *Journal of Sound and Vibration*, vol. 272, pp. 137-154, 2004.